ESRF	**Experiment title:** **Non-equilibrium dynamics at the martensitic transition of shape memory alloys: analyzing microstructural avalanches by coherent X-rays**	**Experiment number**: MA-1873
Beamline: ID10	**Date of experiment**: from: 24.07.2013 to: 31.07.2013	**Date of report**: 05.03.2014
Shifts: 18	**Local contact(s)**: Dr. Federico Zontone	*Received at ESRF:*

Names and affiliations of applicants (* indicates experimentalists):

Dipl.-Phys. Michael Widera*, II Physik. Inst., RWTH Aachen University, D-52056 Aachen, Germany

Prof. Dr. Uwe Klemradt*, II Physik. Inst., RWTH Aachen University, D-52056 Aachen, Germany

Report:

The aim of this experiment was to observe non-equilibrium dynamics in a narrow temperature range near the martensitic phase transition. Non-equilibrium states are related to inner stress fields induced through the phase transition and become noticeable through aging effects and/or incubation time effects.
To elucidate the role of diffusion played in the process, selected model alloys ($Ni_{63}Al_{37}$, $Au_{50.5}Cd_{49.5}$, $Au_{52.5}Cd_{47.5}$) that differ in the ratio of the martensitic transformation temperature M_S to the melting temperature T_M had been selected (see Table 1). The use of X-ray photon correlation spectroscopy and the related one- and two-time-correlation functions allow the direct observation of slow diffusion processes related to martensitic aging. Furthermore, the simultaneous use of an acoustic emission setup, the effect of microstructural avalanches and the impact with respect to the speckle pattern and two-time correlation functions investigated. The experiment was carried out in Bragg reflection geometry to follow the splitting of relevant Bragg peaks during the phase transition. Single crystals with a polished (001) surface were used. The necessary temperature stability of ±3 mK in the temperature range of 230 K to 400 K was provided by a dedicated sample chamber and equipment brought to the experiment. A beam size of 7x7 μm^2 was provided by a pinhole placed 20 cm in front of the sample. The scattered speckle pattern was detected by an Andor CCD camera with a pixel size of 13x13 μm^2 placed 135 cm behind the sample. The X-ray energy was set to 8 keV, to avoid a fluorescence background and to obtain the highest quantum efficiency.

Table 1: Thermodynamic data for the model alloys. The ratio of the martensite-start-temperature to the melting temperature is a figure of merit related to the potential role of diffusion in the corresponding alloy.

Alloy	M_S (K)	T_M (K)	M_S/T_M
$Au_{50.5}Cd_{49.5}$	305	900	0.34
$Au_{52.5}Cd_{47.5}$	330	900	0.36
$Ni_{63}Al_{37}$	298	1793	0.16

In the beginning of each measurement, the sample was heated 35 K above the respective transition temperature. In the vicinity of the martensitic phase transition, the temperature was reduced with a temperature ramp of 0.1 K/min, followed by a waiting time for thermal equilibrium. The added experimental possibility to record acoustic emission of the sample undergoing the phase transition simplified the finding of martensitic start temperatures. The data were taken with a time resolution of 1 s followed by a readout time of ca. 0.67 s. Two-time correlation functions were used to analyze all data.

I. Non-equilibrium dynamics for $Au_{50.5}Cd_{49.5}$

Using two-time correlation functions for isothermal data, non-equilibrium dynamics was clearly observable (see Fig. 1). This is in agreement with previous experimental findings. For quantifiying the results, we used non-averaged one-time correlation functions for slow non-equilibrium dynamics. To include generalized exponential functions, a Kohlrausch-Williams-Watt approach was used. An oscillating stretching exponent with $\beta = 1.93 \pm 0.26$ and a slightly increasing relaxation time ($\tau = (562 \pm 269)$ seconds) were observed. Furthermore, using temperature ramps with 0.1 K/min and isothermal data, microstructural avalanches could be detected using XPCS and acoustic emission. These aspects of the data are not described here and subject of an ongoing doctoral dissertation.

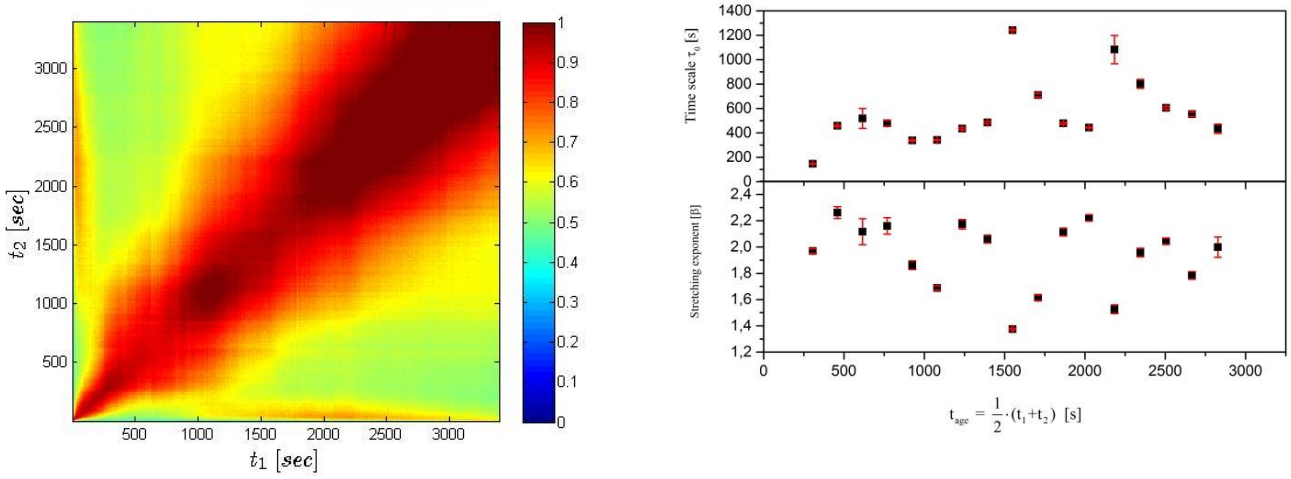

Fig. 1: (left)Two-time correlation function at a temperature of 304 K for $Au_{50.5}Cd_{49.5}$. The divergent color contours provide evidence for non-equilibrium dynamics. Microstructural avalanches could not be observed during this measurment.(right) Sytems parameters describing the acutal slow dynamics.

II. Non-equilibrium dynamics for $Au_{52.5}Cd_{47.5}$

To distinguish between non-ergodic dynamics and strain glass behavior in the AuCd family, also $Au_{52.5}Cd_{47.5}$ has been investigated. Using acoustic emission $Au_{52.5}Cd_{47.5}$ differs completely in the

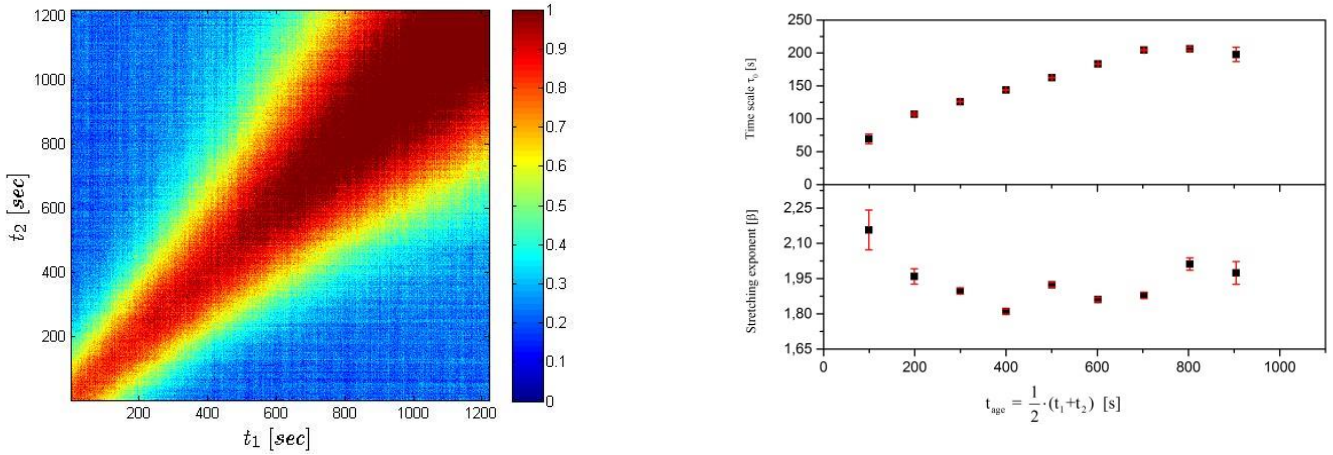

Fig. 2: (left)Two-time correlation function at a temperature of 330 K for $Au_{52.5}Cd_{47.5}$. The divergent color contours provide evidence for non-equilibrium dynamics also in this case. (right) Systems parameters describing the actual slow dynamics.

transformation path in comparison to $Au_{50.5}Cd_{49.5}$. This indicates a significantly different behavior during the martensitic transformation. Since this was the first investigation of the Au-rich type of alloy, overview data had to be taken first. For the first time, non-equilibrium dynamics for $Au_{52.5}Cd_{47.5}$ was measured (see Fig. 2). This finding shows clearly that non-equilibrium dynamics are a common phenomenon in a large family of martensitic alloys. Using non-averaged one-time correlation functions, which depend on the aging time of the system, the KWW parameters yield a nearly stable stretching exponent $\beta = 1.94 \pm 0.11$ and an increasing relaxation time (τ = (155 ± 47) seconds). Furthermore, using temperature ramps with 0.1 K/min and isothermal data, microstructural avalanches were detected using XPCS and acoustic emission. These data are still under evaluation.

III. Non-equilibrium dynamics for $Ni_{63}Al_{37}$

Using two-time correlation functions, non-equilibrium dynamics has been found in $Ni_{63}Al_{37}$. Also the effect of microstructural avalanches could be observed, which are represented by "cuts" in the two-time correlation function (e.g., sudden breakdowns of the correlation). Using non-averaged one-time correlation functions, the KWW parameters yield an oscillating stretching exponent $\beta = 1.79 \pm 0.35$ and an increasing relaxation time (τ = (344 ± 158) seconds).

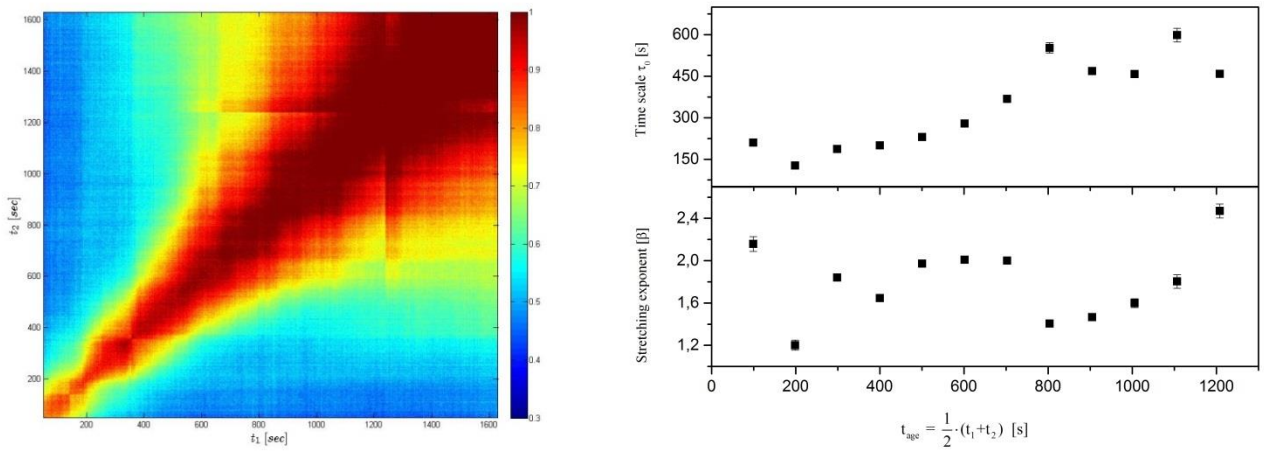

Fig. 3: (left)Two-time correlation function at a temperature of 280 K for $Ni_{63}Al_{37}$. The divergent color contours showing non-equilibrium dynamics. Microstructural avalanches can be observed during the measurement. (right) Systems paramteters describing the actual slow dynamics

IV. Conclusion and outlook

Non-equilibrium dynamics was found in all shape memory alloys investigated in this experiment and quantified using two-time correlation functions. With the use of non-exponential KWW functions, characteristic parameters such as stretching exponents and time constants could be extracted.

- Two different Au-Cd samples were investigated that represent different types of martensitic alloys. The comparison of their characteristic parameters from fits to KWW functions show a similarity regarding the stretching exponents, but a characteristic time scale that differs significantly $Au_{52.5}Cd_{47.5}$: (155 ± 47) seconds, $Au_{50.5}Cd_{49.5}$: (562 ± 269) seconds.
- Non-equilibrium dynamics had been observed in different model alloys, which differ only in the stretching exponent and relaxation time. This leads to the conclusion that diffusion is a common feature in these alloys, which are formally classified as athermal.

Furthermore, the two-time correlation functions show sharp cuts, when microstructural avalanches occur in the part of the sample illuminated by the X-ray beam. For further analysis the avalanche exponents from XPCS will be compared to exponents measured by acoustic emission spectroscopy during the same experiment.